Topographic barriers drive the pronounced genetic subdivision of a range-limited fossorial rodent

Victoria M. Reuber[a], Michael V. Westbury[b], Alba Rey-Iglesia[b], Addisu Asefa[a], Nina Farwig[a], Georg Miehe[c], Lars Opgenoorth[d,e], Radim Sumbera[f], Luise Wraase[g], Tilaye Wube[h], Eline D. Lorenzen[b*] and Dana G. Schabo[a*]

[a] Department of Biology, Conservation Ecology, University of Marburg, Germany

[b] Globe institute, University of Copenhagen, Denmark

[c] Department of Geography, Vegetation Geography, University of Marburg, Germany

[d] Department of Biology, Plant Ecology & Geobotany, University of Marburg, Germany

[e] Swiss Federal Research Institute WSL, Birmensdorf, Switzerland

[f] Department of Zoology, University of South Bohemia, České Budějovice, Czech Republic

[g] Department of Geography, Environmental Informatics, University of Marburg, Germany

[h] Department of Zoological Sciences, College of Natural and Computational Sciences, Addis Ababa University, Ethiopia

* These authors contributed equally to this study

Correspondence: reuber@staff.uni-marburg.de

Keywords: landscape genetics, conservation genetics, population genetics, fossorial rodents, afro-alpine

Abstract

Due to their limited dispersal ability, fossorial species with predominantly belowground activity usually show increased levels of population subdivision across relatively small spatial scales. This may be exacerbated in harsh mountain ecosystems, where landscape geomorphology limits species' dispersal ability and leads to small effective population sizes, making species susceptible to environmental change. The giant root-rat (*Tachyoryctes macrocephalus*) is a highly fossorial rodent confined to the afro-alpine ecosystem of the Bale Mountains in Ethiopia. Using mitochondrial and low-coverage nuclear genomes, we investigated 77 giant root-rat individuals sampled from nine localities across its whole ~1,000 km^2 range. Our data revealed a distinct division into a northern and southern subpopulation, with no signs of gene flow, and higher nuclear genetic diversity in the south. Landscape genetic analyses of the mitochondrial genomes indicated that population subdivision was driven by steep slopes and elevation differences of up to 500 m across escarpments separating the north and south, potentially reinforced by glaciation of the south during the Late Pleistocene (~42,000 to 16,000 years ago). Despite the pronounced subdivision observed at the range-wide scale, weak geographic structuring of sampling localities within subpopulations indicated gene flow across distances of at least 16 km, suggesting aboveground dispersal and high mobility for relatively long distances. Our study highlights how topographic barriers can lead to the genetic subdivision of fossorial species, despite their potential to maintain gene flow at the local scale. These factors can reduce genetic variability, which should be considered when developing conservation strategies.

1. Introduction

The genetic subdivision and diversity of a species across space are determined by the combined effects of the environment and the ability of a species to disperse (Berthier et al., 2005; Manel et al., 2012; Quaglietta et al., 2013; Ruiz-Gonzalez et al., 2015). Dispersal ability can be limited by topographic barriers such as mountains or steep slopes, and by species-specific abiotic or biotic requirements, such as temperature or food availability, which may prevent the continuous distribution of individuals and reduce gene flow (Boulangeat et al., 2012; Cunningham et al., 2016; Cushman & Lewis, 2010; Sexton et al., 2009). As a consequence, natural selection, genetic drift, and inbreeding in smaller isolated populations may lead to heterogeneous patterns of genetic variability and population subdivision (Wright, 1969). Species with low dispersal ability such as those with low mobility and a burrowing lifestyle, are especially prone to these processes.

Fossorial rodents engineer elaborate underground burrow systems. In many species, activities including searching for mates, reproduction, and foraging, occur below-ground (Nevo, 1999). Therefore, these rodents are often restricted to specific soil types and available food resources (Begall et al., 2007; Nevo, 1999; Reichman, 1975). Apart from these notable constraints in habitat and resource availability, the low mobility of fossorial species leads to small home ranges and limited dispersal (Harestad & Bunnel, 1979; Tucker et al., 2014). As a result, fossorial rodents often have a localised and patchy distribution. Moreover, in the case of solitary species, mature individuals meet mainly during the mating season, which further limits conspecific encounters. Combined, these characteristics lead to small and isolated subpopulations, with low genetic variation and genetic differentiation across relatively small scales and rapid inter-population divergence, as shown for instance in several tuco-tuco species (*Ctenomys sp.,*) and common voles *(Microtus arvalis)* (Mapelli et al., 2012; Mirol et al., 2010; Nevo, 1999; Schweizer et al., 2007).

These genetic and ecological patterns may be exacerbated in harsh environments, such as in mountain ecosystems, where the geomorphology of the landscape and the availability of suitable

habitats, limits dispersal opportunities and leads to restricted species distribution ranges and small effective population sizes (Badgley et al., 2017; Brown, 2001; Gaston, 2003; Rahbek, Borregaard, Colwell, et al., 2019). As a result, mountain regions have been recognized as hotspots for genetic differentiation and speciation, contributing disproportionately to terrestrial biodiversity, at least in the tropics (Rahbek, Borregaard, Antonelli, et al., 2019; Rahbek, Borregaard, Colwell, et al., 2019; Sandel et al., 2011). However, species with limited distribution ranges and small population size, such as those found in mountain ecosystems, are at particular risk of extinction (Davies et al., 2009; Gaston, 2003). Small populations tend to exhibit accumulations of deleterious mutations, low intraspecific diversity, or loss of adaptive potential, making them susceptible to environmental change and habitat shifts (Hoffmann et al., 2017; Lande, 1988; Willi et al., 2006). Additionally, upslope habitat shifts are limited for mountain species, especially for those occurring near mountaintops (Parmesan, 2006; Wilson & Gutiérres, 2016). Mountain ecosystems face increasing threats from land use and climate change-induced habitat shifts. Therefore, it is imperative to understand the impact of species-environment interactions on genetic diversity to effectively establish conservation targets, however, thorough understanding is still lacking. Studying species in mountain ecosystems remains a challenge, especially for fossorial rodents, due to the difficulty of accessing remote areas and the inherent challenges in assessing these species in their natural habitats.

Our study addresses this knowledge gap by elucidating how landscape features drive the genetic subdivision and diversity of the giant root-rat (*Tachyoryctes macrocephalus*), a fossorial rodent endemic to the afro-alpine and afro-montane ecosystem of the Bale Mountains in southeast Ethiopia (Figure 1). The species has a limited distribution range of ~1,000 km^2 across the Bale Mountains massif and is found between 3,000 and 4,150 m above sea level (a.s.l.) (Sillero-Zubiri et al., 1995; Yalden & Largen, 1992). Giant root-rats have specific habitat requirements, occurring in grasslands in areas with good soil depth, especially along wetland shores and flooded valleys (Sillero-Zubiri et al.,

1995; Šklíba et al., 2017). Grassland in river valleys that spread through shrubs and forest zones into lower elevations, allow the species to expand down to about 3,000 m a.s.l. (Yalden, 1985). Their relatively small home ranges (about 100 m^2) can shift throughout the year depending on food availability (Šklíba et al., 2020). Giant root-rats are significant ecosystem engineers creating large underground burrow systems, in which they live solitarily. Through their combined effect of soil perturbation and herbivory, they alter nutrient availability, soil texture and moisture, and create their own habitat and that for other plant and animal species (Asefa et al., 2022; Miehe & Miehe, 1994; Šklíba et al., 2017; Yalden, 1985). By using below-ground burrows, the species circumvents the harsh environmental conditions of the mountain ecosystem, which include strong winds and temperatures below 0 C°, and limits the risk of being preyed upon by its main predator the Ethiopian wolf (*Canis simensis*) (Sillero-Zubiri & Gottelli, 1995; Šumbera et al., 2020; Vlasatá et al., 2017; Yalden, 1985). Taken together, the species' key role as ecosystem engineer combined with its limited range in a changing mountain ecosystem, makes it an ideal model organism for investigating the connection between genetic patterns and landscape features, so as to preserve mountain biodiversity and ensure ecosystem functioning.

In the present study, we analysed the spatial genetic subdivision and diversity in the giant root-rat across its distribution range. To achieve this, we analysed both mitochondrial genomes (mitogenomes) and nuclear genomes, and further utilized mitogenomes to investigate the relationship between genetic differentiation and landscape features. We generated complete mitogenomes and low-coverage nuclear genomes from 77 individuals collected across nine sampling localities in the Bale Mountains (Figure 1). We applied two different landscape genetic approaches to evaluate how mitochondrial gene flow of the species is impacted by geographic distance, by vegetation and soil moisture (used as proxies for food and soil availability), and by slope and elevation (used as proxies for topographic barriers). Due to the predominantly below-ground activity and patchy distribution of the giant root-rat, we hypothesise strong genetic subdivision across small

125 spatial scales. Owing to the pronounced heterogeneity of the environment in the Bale Mountains, we
126 hypothesise that genetic structuring is driven by habitat availability, and by topographic structures
127 across the species' range.

128 **2. Materials and method**

129 **2.1 Study area**

130 The Bale Mountains in southeast Ethiopia (6º29'N – 7º10'N and 39º28'E – 39º57') represent Africa's
131 largest afro-alpine ecosystem, comprising ~8 % of the continent's area above 3,000 metres above sea
132 level (m a.s.l) (Groos et al., 2021, Figure 1A-C). In order to protect the unique afro-montane and afro-
133 alpine ecosystem of the Bale Mountains, the area above ~3,200 m a.s.l. became a national park in
134 1970. The Bale Mountains are characterised by two rainy seasons and one dry season per year, with
135 short rains from March to June, long rains from July to October, and a dry season from November to
136 February. The vegetation of the Bale Mountains shows an elevational zonation from moist montane
137 forest (~1,500 - 3,500 m a.s.l.) over ericaceous shrubland and dwarf forest (~3,500 - 4,000 m a.s.l.) to
138 afro-alpine vegetation with open grassland and *Erica* outposts (above 4,000 m a.s.l.). Dwarf-scrub
139 vegetation, such as *Helichrysum* associated with *Lobelia*, is the main plant formation in the afro-
140 alpine vegetation but does not cover the whole area, leaving open spaces for herbaceous plants like
141 *Senecio*, *Alchemilla* or *Salvia* (Miehe & Miehe, 1994; Tallents & Macdonald, 2011)

142 Characteristic of the Bale Mountains National Park is the afro-alpine Sanetti Plateau, which
143 spans elevations from approximately 3,800 m a.s.l, to 4,377 m a.s.l. at the peak of the mountain Tullu
144 Dimtu (Figure 1C). Large parts of the plateau were glaciated during the Late Pleistocene, between
145 42,000 to 16,000 years ago (Groos et al., 2021). The plateau is bounded by several outlet valleys in
146 the north and the east with slopes that are covered by dense, shrubby *Erica* vegetation and by
147 congealed lava flows at its northwestern margins. These topographic structures distinguish the

148 plateau from the northern region of the national park, which is ~300 - 500 m lower in elevation and
149 comprises broad valleys and plains with afro-alpine vegetation (Miehe & Miehe, 1994). In
150 comparison to the plateau, the north has higher moisture availability and milder temperatures.

151 **2.2 Sampling**

152 We collected tissue samples from 77 live giant root-rat individuals at nine localities across the Bale
153 Mountains National Park, covering the distribution range of the species (Figure 1C, supporting
154 information Table S1). The sampling localities were distributed across the two topographically
155 distinct regions in the national park, in the north (localities N1-N3) and in the south (localities S1-S6).
156 The southern localities are scattered across the centre and south of the Sanetti Plateau. Localities
157 sampled in the north of the plateau lie at a lower elevation (~3,500 m a.s.l) than localities sampled in
158 the south (~3800 - 4000 m a.s.l.). Sampling localities between regions were separated by 15.3 to 28.3
159 km, and localities within regions were separated by 2.6 km to 16.0 km.

160 We captured 7-9 giant root-rat individuals per locality (except locality S4 with n=1). The samples
161 were collected in January and February in two consecutive years (2020, 2021) under the permit of
162 the Ethiopian Wildlife Conservation Authority. Individuals were caught with snare traps that were
163 monitored by the capture team at all times to guarantee no harm to the animals. A ~0.5 cm^2 piece of
164 skin from the hind leg was cut with sterilised scissors and stored in 96% ethanol or DNAgard® for
165 blood and tissue (Biomatrica, Inc.) for genomic analyses. After sterilising the wound, the animals
166 were immediately released back into their burrow systems.
167

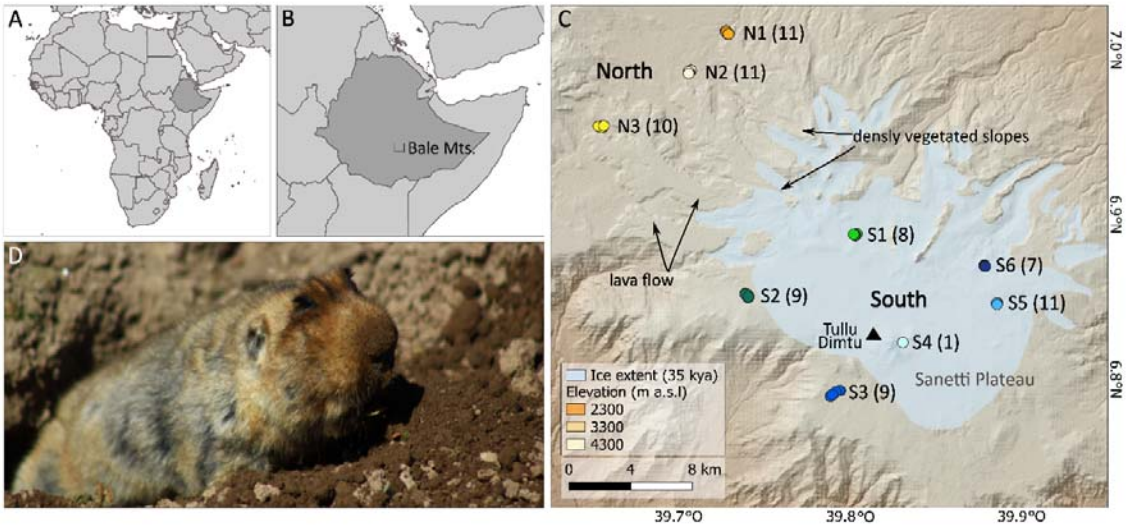

Figure 1: Sampling localities of giant root-rats within Bale Mountains National Park, Ethiopia. A) Map of Africa showing Ethiopia in dark grey; B) Map of Ethiopia indicating location of Bale Mountains National Park, C) Map of the nine sampling localities from two distinct geographic regions. The north (~3,500 m above sea level [m a.s.l]), and south (~3,800-4,000 m a.s.l, Sanetti Plateau) are separated by steep slopes covered with dense Erica thickets and congealed lava flows. Sample size of each locality is indicated in brackets. Tullu Dimtu is the highest peak in the Bale Mountain National Park at 4,377 m a.s.l., and is indicated with a filled triangle. Region with light blue shading indicates the glacial extent within Bale Mountains National Park ~35±7.1 thousand years ago (kya) (Groos et al., 2021; Ossendorf et al., 2019); D) Burrowing giant root-rat, photography by V. Reuber.

2.3 Laboratory analyses

We extracted DNA from the tissue samples using the Qiagen DNeasy® Blood and Tissue Kit following the manufacturer's protocol (Qiagen Ltd.). 60 of the samples were processed in-house in the modern DNA labs at Globe Institute, University of Copenhagen. The DNA concentration of the extracts was measured using QubitTM dsDNA HS (Invitrogen). After quantification, we diluted the extracts to a concentration of 6 ng/µl in a total volume of 50 µl. DNA was sheared to ~400 base pair (bp) fragment lengths using the Covaris M220 ultrasonicator. We built DNA fragments into an Illumina library following the protocol from Carøe et al., (2018) and double-indexed them using AmpliTaq Gold Polymerase (ThermoFisher) during the indexing PCR step. Index PCR reactions were performed in 100 µl, using 1x PCR buffer, 2.5 mM of MgCl (25 mM), 0.2 mM of dNTPs (25 mM), 0.2 µM of index primer mix (10 µM), and 0.1 U/ µl of polymerase (5 U/µl). PCR cycling conditions were 95 °C for 10 min; 10 -

188 18 cycles of 95 °C for 30 s, 50 °C for 30 s and 72 °C for 1 min followed by 72 °C for 5 min. The number
189 of cycles for the index PCR was determined from qPCR analysis. Post-amplification, libraries were
190 purified using SPRI beads as in Carøe et al., (2018). The purified indexed libraries were quantified on
191 a QubitTM dsDNA HS (Invitrogen), and quality-checked on either an Agilent 2100 Bioanalyser or an
192 Agilent Fragment AnalyzerTM. Libraries were pooled equimolarly and sequenced on an Illumina
193 NovaSeq 6000 using paired-end (PE) 150 bp technology (Novogene Europe,
194 http://en.novogene.com).

195 For the remaining 17 samples, DNA was extracted and processed to libraries by Novogene and
196 sequenced on a NovaSeq 6000, using paired end 150 bp technology.

197 **2.4 Data generation of mitochondrial and nuclear DNA**

198 We trimmed adapters and removed reads shorter than 30 bp for each individual using skewer v0.2.2.
199 (Jiang et al. 2014). We merged overlapping paired-end reads using FLASHv1.2v11 (Magoč & Salzberg,
200 2011) with default parameters. We mapped both merged and unmerged reads to the hoary bamboo
201 rat (*Rhizomys pruinosus*) nuclear genome (Genbank accession: VZQC00000000.1; Guo et al., 2021)
202 which is the nearest relative of the giant root-rat with an available genome, combined with the giant
203 root-rat mitogenome (Genbank accession: MW751806; Reuber et al., 2021). We used BWA v0.7.15
204 (Li & Durbin, 2009) utilising the mem algorithm and default parameters. We parsed the alignment
205 files, and removed duplicates and reads of mapping quality score <30 using SAMtools v1.6 (Li et al.,
206 2009). We built consensus mitogenomes from each individual using a majority rules approach (-
207 doFasta 2) in ANGSD v0.921 (Korneliussen et al., 2014) only considering bases with a base quality
208 score greater than 30 (-minq 30), reads with a mapping quality score greater than 30 (-minmapq 30),
209 and sites with at least 10x coverage (-minInddepth 10). The mitogenomes are available under
210 GenBank accessions OQ207545 - OQ207620.

2.5. Genetic subdivision

2.5.1 Mitochondrial DNA analysis

Haplotype network

The mitogenomes were aligned with Mafft v.7.392 (Katoh & Standley, 2013). We constructed a median-joining haplotype network to investigate the relationships among the 77 mitogenomes using the software PopArt v.1.7 (Leigh & Bryant, 2015).

Phylogenetic analysis

We constructed a Bayesian phylogeny with the 48 mitogenome haplotypes identified in the network analyses, using MrBayes v.3.2.7a (Ronquist & Huelsenbeck, 2003). We used the GTR + I + G model of evolution, which was defined as the best model with PartitionFinder v. 2.1.1 (Lanfear et al., 2017) prior to the analysis. The MCMC algorithm was run twice with four chains of 10 million generations, sampled every 1,000 generations and with a 10 % burn-in. The trees were combined following the majority-rule consensus approach, to assess the posterior probability of each clade. The resulting tree was visualised in FigTree v.1.4.4 (http://tree.bio.ed.ac.uk/software/figtree/; supporting information Figure S1).

Fixation statistics and AMOVA

We calculated the pairwise differentiation between eight of the nine sampled localities (omitting S4 as n=1) with the F_{ST} -estimator of the software Arlequin v. 3.5.2.2 with 10,000 permutations (Excoffier & Lischer, 2010); *p*-values of F_{st} estimates were adjusted using the Bonferroni correction (Rice, 1989), controlling for a false-positive discovery rate (R Core Team, 2021). Additionally, we conducted a hierarchical analysis of molecular variance (AMOVA), also in Arlequin, with localities grouped into their provenance in the regions north and south (Figure 1C).

235 2.5.2 Nuclear DNA analysis

236 We investigated population subdivision of the nuclear data using principal component analysis (PCA)
237 and admixture proportion analysis. We generated genotype likelihoods in ANGSD (Korneliussen et
238 al., 2014) for all individuals using the following filters and parameters: call genotype likelihoods using
239 the GATK algorithm (-GL 2), output a beagle file (-doGlf 2), only include reads with mapping and base
240 qualities greater than 30 (-minmapQ 30 and -minQ 30), only include reads that map to one location
241 uniquely (-uniqueonly 1), a minimum minor allele frequency of 0.05 (-minmaf 0.05), only call a SNP if
242 the p-value is greater than $1e^{-6}$ (-SNP_pval 1e-6), infer major and minor alleles from genotype
243 likelihoods (-doMajorMinor 1), only include sites if at least 40 individuals are covered (-MinInd 40),
244 remove scaffolds shorter than 100 kb (-rf), and remove secondary alignments (-remove_bads 1). To
245 compute the PCA, we constructed a covariance matrix from the genotype likelihoods using PCAngsd
246 v0.98 (Meisner & Albrechtsen, 2018). Admixture proportions were calculated using the same
247 genotype likelihoods with NGSadmix (Skotte et al., 2013). We ran NGSadmix specifying K=2 and K=3.
248 To evaluate the reliability of the NGSadmix results, we ran each *K* up to 100 times independently. If
249 we retrieved consistent log-likelihoods from at least two independent runs, the corresponding K was
250 considered reliable.

251 To estimate levels of differentiation among localities, we computed F_{ST} from a consensus haploid
252 call file created using ANGSD (-dohaplocall 2) and the same filtering parameters as the PCA and
253 admixture proportions above. We calculated the F_{ST} using an available python script
254 https://github.com/simonhmartin/genomics_general/blob/master/popgenWindows.py) and
255 specifying a window size of 1Mb, and a minimum number of sites per window as 1,000 bp.

256

257 *Gene flow*

258 The mitogenomes of two individuals (WM07 from locality S1 and GG01 from locality S6) grouped
259 with individuals from the north in the haplotype network and phylogeny. We therefore used D-

statistics (also known as ABBA/BABA, Durand et al., 2011) to test whether the results were driven by ancient gene flow between regions north and south, or by incomplete lineage sorting. We tested several topologies [[H1, H2], H3], with branch H1 being one of the two putative introgressed individuals, and branches H2 and H3 being individuals from one region north or south, or one from each region. A negative D-score illustrates a closer relationship between H1 and H3 than H2 and H3, while a positive D-score indicates that branches H2 and H3 are more closely related than H1 and H2. This setup can also be used to uncover population subdivision, as the incorrect input topologies would lead to elevated D-scores due to more recent common ancestry, as opposed to gene flow (Westbury et al., 2018).

We performed the D-statistic tests using a random base-call approach in ANGSD (-doAbbababa 1). We implemented the same filtering approach as for the above analyses but only included scaffolds >1 megabase (Mb) in size, a block size of 1 Mb (-blocksize 1000000), and the hoary bamboo rat (*Rhizomys pruinosus*, GenBank accession VZQC00000000.1, Guo et al., 2021) as the ancestral state/outgroup (-anc). To assess the significance of our results we used a block jackknife test with the script jackKnife.R which is available with the ANGSD tool suite.

2.6 Diversity

Based on the mitochondrial genomes, we calculated nucleotide diversity (π) per region, and separately for eight of the nine localities using DnaSp v.6 (omitting S4 as n=1) (Rozas et al., 2003). We tested differences in nucleotide diversity between the two geographic regions, and among localities using genetic_diversity_diffs v. 1.0.3 (Alexander, 2017).

The python script used to calculate nuclear F_{ST} above simultaneously computes nucleotide diversity per region and per locality. To test for significant differences in levels of nucleotide diversity between regions and between localities, we used a Welch-test (unpaired t-test), accounting for unequal variance.

284 **2.7 Landscape genetic analysis**

285 We applied two landscape genetic approaches to investigate the effects of landscape features on the
286 observed genetic differentiation between localities based on F_{ST} estimates of the mitogenomes. We
287 exclusively used mitogenomes due to their higher mutation rates and lack of recombination
288 compared to nuclear genomes, which result in faster responses to environmental changes and
289 increased resolution (Avise, 2000; Birky et al., 1983). The limited number of sampling localities
290 prevented us from analysing the north and south regions separately.

291 We selected four environmental variables (vegetation, soil moisture, slope, elevation), which
292 were based on satellite-based remote sensing data, as predictors for genetic differentiation of the
293 giant root-rat. For vegetation and soil moisture, we used observations from satellite Sentinel-2,
294 captured on an almost cloud-free day on December 15, 2017, and derived from the USGS Earth
295 Explorer repository. We used the red, green, blue, red and near infrared bands of from the Sentinel-2
296 observations and with those computed raster layers of the Normalised Differentiation Vegetation
297 Index (vegetation index) and Land-Surface Water Index (soil moisture index, for details see Wraase et
298 al., 2022) using the Rtoolbox, as proxies for food and soil availability for giant root-rats (Sillero-Zubiri
299 et al., 1995; Šklíba et al., 2017; Yaba et al., 2011; Yalden & Largen, 1992). To determine whether
300 topographic structures act as barriers for burrowing giant root-rats, we included the variables slope
301 and elevation in our analysis. Raster layers for slope and elevation were obtained from a Shuttle-
302 Radar-Topography-Mission digital elevation model from the USGS Earth explorer
303 (www.earthexplorer.usgs.gov). The generated raster layers of all four environmental variables had a
304 30 x 30 m resolution and were cropped on extent 567910.0, 605990.0, 738620.0, 778750.0. Our
305 analyses were conducted in R environment version 4.2.1 (R Core Team, 2021).

306

307 *Partial Mantel tests*

Using partial Mantel tests, we analysed if the genetic differentiation between eight of the nine sampling localities (omitting S4 as n=1) was correlated with geographic distance, vegetation, soil moisture, slope and elevation (see above). Therefore, we constructed distance matrices. The genetic distance matrix was generated by linearizing the pairwise genetic differentiation estimates between localities, i.e the F_{ST} -estimates ([F_{ST} /(1- F_{ST})]; Rousset, 1997). The geographic distance matrix was calculated in Euclidean distances and log-transformed to linearize the relationship with genetic distance. For each environmental variable, we extracted their values from the computed raster layers at the coordinates of the sampling localities and therewith generated the environmental distance matrices. We then applied a pairwise reciprocal causal modelling approach. Reciprocal causal modelling compares partial Mantel tests of a focal environmental model, removing the influence of a competing, alternative model (Cushman et al., 2006; Cushman & Landguth, 2010). In this approach, the correlation between one environmental distance matrix and genetic distance is controlled by a second matrix (e.g. focal model: genetic distance~geographic distance|elevation distance) and in a next step, both environmental distance matrices are interchanged (e.g. alternative model: genetic distance~elevation distance|geographic distance). In that way, we were able to account for high correlation among matrices (Cushman et al., 2006; Cushman & Landguth, 2010). To assess which of the two models explains genetic distance better, the relative support of the focal and alternative model was calculated by estimating the difference between the correlation values of the two models. If the difference in correlation factors was positive, we assumed that the focal hypothesis was correct. The partial Mantel tests were performed with 9,999 permutations in the vegan R package v.2.6-4. (Oksanen et al., 2020).

Raster layer optimization framework to generate resistance surfaces

We used a raster layer optimization framework developed by Peterman et al. (Peterman, 2018; Peterman et al., 2014), to further identify landscape features that explain mitochondrial genetic

differentiation, using the R package ResistanceGA (Peterman, 2018). In this framework, the raster layers of the environmental variables (see above) were transformed into resistance surfaces, with the ResistanceGA package utilising a genetic algorithm from the GA R package (Scrucca, 2013). A resistance surface is a spatial layer that assigns values to each grid in the raster layer of the selected environmental variable. Those values are used to estimate the cost of dispersal and mirror to what extent the selected variable hinders or facilitates the connectivity of a species between two localities (pairwise resistance distances). Thereby, there are no *a priori* assumptions about the relationship between the environmental variable and the species' dispersal characteristics. The genetic algorithm in the optimization framework is used to maximise the relationship between the resistance distances of each raster layer, and the pairwise genetic differentiation (F_{ST}) between localities. The process of generating resistance surfaces is repeated, and in every iteration, the resistance distances are fitted against the genetic distances in a mixed effect model, until the objective function, the AIC (Akaike's information criterion; Akaike, 1974) of the mixed effect model does not improve further. The mixed-effect models are conducted using a maximum likelihood population effect parameterization to account for the non-independence of the predictor variables and to account for spatial autocorrelation (Clarke et al., 2002; Peterman et al., 2014; Shirk et al., 2018). This iterative process works towards identifying the best-fit landscape resistance surface.

In our optimization framework, we used a single surface optimization approach, where the resistance surfaces of the raster layers of each selected environmental variable (i.e. vegetation index, soil moisture index, slope and elevation) were optimised individually, using eight transformation functions (Monomolecular and Ricker functions) and the default parameters (Peterman, 2018). In this step, the pairwise resistance distance between localities was estimated by assuming that individuals can use several paths to disperse. Resistance distances were generated with the *costDist* function implemented in the ResistanceGA package and movements between localities were allowed in eight directions during resistance distance calculation. Because Euclidean distance is incorporated

in the resistance distances, it was not included as an additional variable. In the optimization process, the mixed-effect models were calculated, fitting the pairwise genetic differentiation as a response against the resistance distances as single fixed effects, using the AIC for model evaluation and including sampling localities as a random effect to account for spatial autocorrelation. We did two independent optimization runs to confirm convergence across runs. The run containing the mixed-model with the greatest log-likelihood value is presented in the results section (Table 1). After the optimization, we used bootstrap model selection with 75% of the samples and 10,000 iterations. The bootstrap model selection refits the mixed-effect models and calculates fit statistics for each model, showing the average AIC and percentage each resistance surface has been selected as a top rank model across all bootstrap iterations (Peterman, 2018).

3. Results

We generated complete mitogenomes from all 77 giant root-rat individuals, with a depth of coverage ranging between 24.94x and 383.22x, and a length of 16,646 bp. For the nuclear genomes, we obtained coverages ranging from 0.12x to 0.77x (supporting information Table S2).

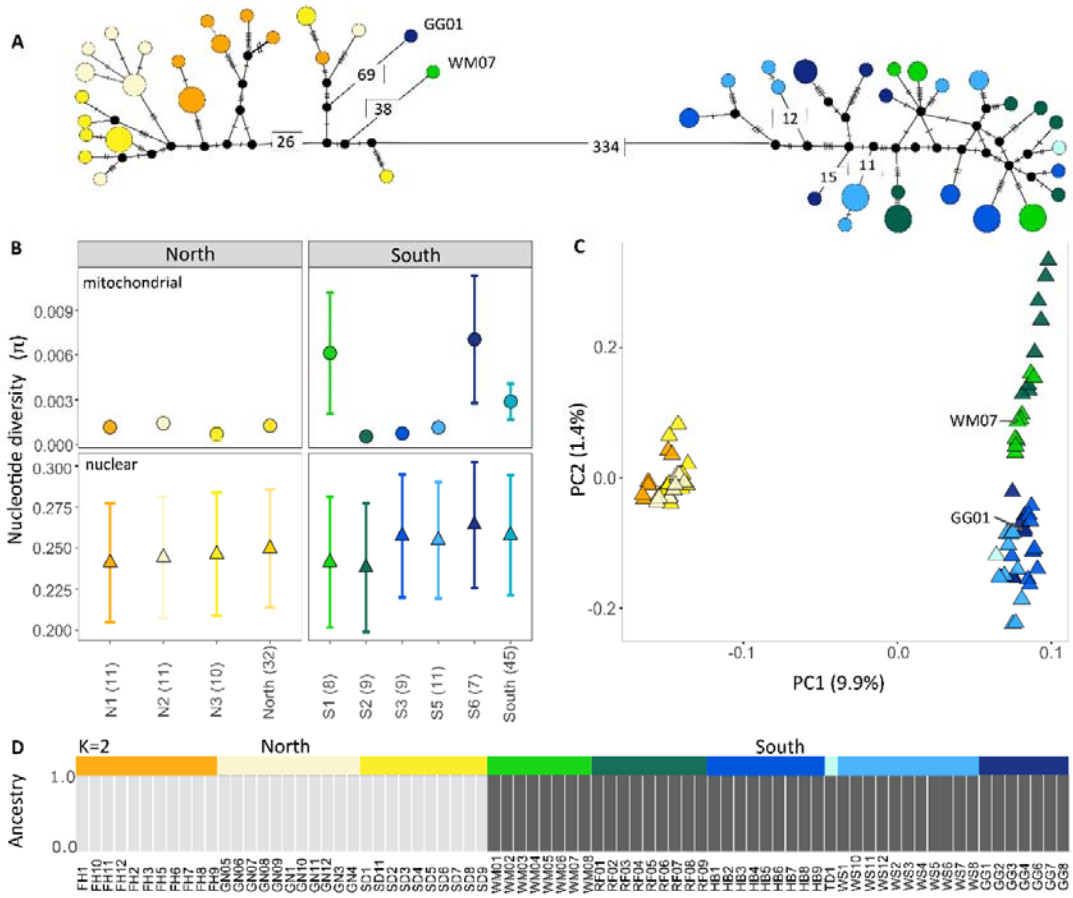

Figure 2: Patterns of genetic diversity and subdivision of giant root-rats across their range. A) Network of the 48 mitochondrial haplotypes present among the 77 sampled individuals. Each circle represents a haplotype, and the relative size of each circle represents haplotype frequency. Numbers on branches show the number of segregating sites between haplotypes for >10. Black dots indicate intermediate haplotypes not present in the data. Distances between haplotypes are not to scale. B) Diversity levels within the sampled localities and subpopulations based on mitogenomes (circles) and nuclear data (triangles). Sample sizes are shown in brackets. C) PCA based on 77 low-coverage nuclear genomes. The percentage of the diversity of each principal component is shown in brackets. D) Ancestry proportions based on the nuclear data for K=2, with each vertical bar representing an individual.

3.1 Genomic analysis

Haplotype network and phylogeny

Our 77 sampled giant root-rat individuals comprised 48 haplotypes, with no haplotypes shared among localities (Figure 2A). The haplotype network and phylogeny of the mitogenomes revealed two geographically separated and well-supported groups; one group comprising all samples collected

388 in the north, with the inclusion of individuals WM07 and GG01 from the south, and one group
389 comprising all other samples from the south (supporting information Figure S1). In the network, we
390 identified 574 segregating sites among individuals, and the northern and southern haplogroups were
391 separated by 334 segregating sites (Figure 2A). The north contained 21 haplotypes (32 individuals)
392 and the south contained 27 haplotypes (45 individuals). Within the north, we identified two distinct,
393 well-supported genetic clades, N_A and N_B (supporting information Figure S1). Clade N_A comprised six
394 individuals (five haplotypes) from localities N1-N3. Individual GG01 from locality S6 was basal to the
395 clade. Clade N_B comprised the remaining individuals from the north with individual WM07 from the
396 south at basal position. We did not identify any spatial genetic structuring in the south.
397 The AMOVA yielded a high level of between-region variation when the eight localities (omitting
398 S4 with n=1) were grouped into north and south (89.50 %, $p < 0.01$). Within each region, the
399 variation was higher within localities (9.27 %) than among localities (1.24 %).
400
401 *Principal component analysis and admixture proportions*
402 We identified two main groups in the nuclear data, in agreement with the mitochondrial findings
403 (Figure 2). In the PCA, individuals from the north separated from the individuals from the south, with
404 almost 10% of the variation explained on the first principal component. The southern group showed
405 a slight separation on the second component, with the more central localities S1 and S2 segregating
406 from the localities further southeast, with 1.4 % variation explained (Figure 2C). The division of the
407 data into north and south was also evident in the admixture analysis of K = 2 (Figure 2D). The
408 admixture analysis did not converge with K = 3, suggesting K = 3 did not reliably fit the data.
409
410 *Gene flow*
411 To investigate the origin of the mitochondrial lineages, present in individuals WW07 and GG01,
412 which were more closely related to the northern haplogroup than the south (Figure 2A), we tested

for ancient gene flow using the nuclear data. Using the topology [[WM07, south], north], we found most comparisons to have a D-score around 0 and a Z-score<|3|, indicating that WM07 and all individuals from the south were equally related to the northern individuals (Figure 3). We found positive D-scores (Z-score>3) when using the topology [[WM07, north], north], demonstrating a closer relationship between individuals from the north with each other than with WM07, which agrees with their more recent common ancestry and the basal position of WM07 in the phylogenetic tree (supporting information Figure S1). We found qualitatively the same results when we investigated the relationship of GG01 (sampled in locality S6) with individuals from the north and south (Figure 3). Hence our analysis did not support that the mitochondrial lineages in WM07 and GG01 were the result of recent gene flow between north and south.

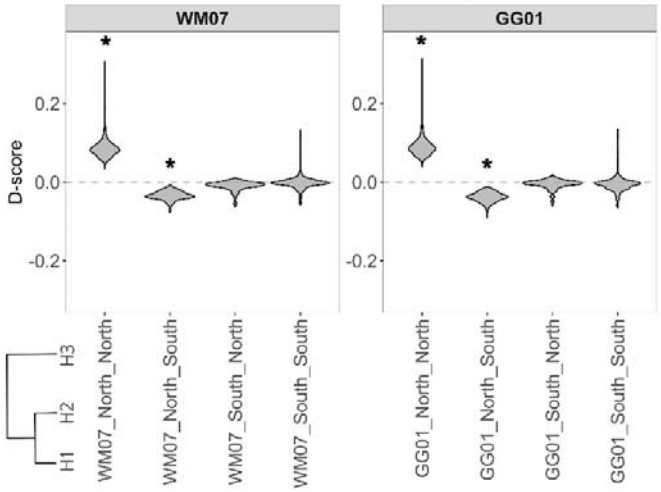

Figure 3: Analysis of signals of gene flow between individuals WM07 from locality S1 and GG01 from locality S6 and their source group in the south, using D-statistics. Negative D-scores suggest gene flow or recent common ancestry between H1 and H3 relative to H2 and H3, while positive D-scores suggest gene flow or recent common ancestry between H2 and H2 relative to H1 and H3. Statistical significance is indicated by asterisks (*) next to scores, when |Z| greater than 3 (supporting information Figure S2), determined by a one-sample Wilcoxon signed rank test.

Genetic differentiation among localities

Investigating pairwise genetic differentiation between localities, we found that F_{ST} - estimates were higher between regions than within regions, at both the mitogenome and nuclear level (Figure 4). For

the mitogenomes, pairwise differences between localities of different regions ranged from 0.82 to 0.97 and were much higher than within regions, where values ranged from 0.09 to 0.29.

For the nuclear data, pairwise F_{ST} - estimates between localities from different regions ranged from 0.04 to 0.06 and were higher than values between localities within regions, which ranged from 0.01 to 0.02 (Figure 4).

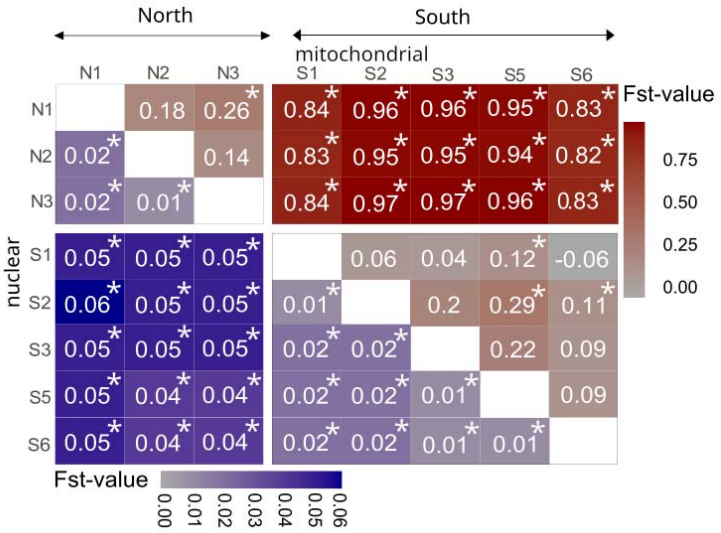

Figure 4: Levels of genetic differentiation between the sampled giant root-rat localities from the north and south of Bale Mountains National Park. Mitochondrial (red, above diagonal) and nuclear (blue, below diagonal) F_{ST}-estimates. * in cells indicates significant differences (*p*-values < 0.05), derived by permuting haplotypes between localities for mitochondrial data and by applying a one-sample t-test on F_{ST} -values for the nuclear data.

Diversity

We estimated levels of diversity for each region, and for each locality (omitting S4 as n=1). For the mitogenomes, diversity in the south ($\pi = 0.003 \pm 0.0002$) was significantly higher than in the north ($\pi = 0.001 \pm 0.001$, $p < 0.05$; Figure 2B), which reflected the presence of the divergent mitochondrial lineages in individuals WM07 and GG01 from localities S1 and S6 (Figure 2A). Thus, this was also apparent in localities S1 and S6 having the highest diversity levels, with S6 showing significantly

452 differentiated levels of diversity ($p < 0.05$) and S1 showing marginal significant differentiation ($p >$
453 $0.05 < 0.1$, supporting information Table S3) to the remaining localities in the south.

454 Based on the nuclear data, we also observed significantly higher diversity in the south ($\pi = 0.257$
455 ± 0.0364) than in the north ($\pi = 0.249 \pm 0.0357$, $p < 0.05$; Figure 2B). Among localities in the south,
456 the two central localities S1 and S2 had lower diversity levels than the localities sampled further to
457 the southeast (S3, S5, S6). All localities had significantly differentiated levels of diversity ($p < 0.05$,
458 supporting information Table S3).

459 **3.2 Landscape genetics**

460 We used a reciprocal causal modelling approach with partial Mantel tests to relate genetic
461 differentiation to the environmental distance matrices of the selected variables (vegetation index,
462 soil moisture index, slope and elevation). Analysing levels of differentiation estimated for each region
463 we found that elevation was the strongest model. Elevation was significantly related to genetic
464 differentiation in all partial Mantel tests, regardless of the second environmental distance matrix
465 controlling elevation (supporting information Table S4 A). Further, elevation showed the strongest
466 relative support; all relative correlation values were positive, after the effect of the other
467 environmental models were removed (supporting information Table S4 B). Geographic distance
468 showed a significant relation with genetic differentiation when controlled by vegetation index, soil
469 moisture index or slope, but was non-significant and the relative correlation value was negative,
470 when controlled by elevation. We could not find significant effects of vegetation, soil moisture or
471 slope on genetic differentiation; all variables had non-significant Mantel correlation values, showing
472 the least support in the reciprocal causal modelling matrix (supporting information Table S4).

473 The raster layer optimization approach revealed that slope and elevation were the best-fitting
474 models for explaining genetic differentiation. Slope was selected as top model in 71%, and elevation
475 in 29% of the times across 10,000 bootstrap iterations (Table 1). The average weight from the

476 bootstrap analyses supported geographic distance as a driver for genetic differentiation, while the
477 parameters rank, AIC, maximum likelihood and R^2 suggested slope and elevation as the best models
478 (Table 1). The the response curve of the optimised resistance surface showed that the resistance
479 costs increased with increasing slope (supporting information Figure S3 C). As in the partial Mantel
480 tests, we could not identify a contribution of the vegetation index or soil moisture index to genetic
481 differentiation (Table 1).

482 Table 1: Model selection results for linear mixed-effect models, testing the effect of resistance distances
483 (dispersal costs based on environmental condition) on levels of mitochondrial genetic differentiation (F_{ST}) in the
484 giant root-rat. The parameters were calculated based on 10,000 bootstrap iterations using a random
485 resampling of 75% of the sampled populations. Frequency top-model percentage, higher average weight and
486 log-likelihood (LL), and lower average rank indicate the best supported models.
487

Resistance distance matrix	Average AIC	Average R^2m	Average LL	Average weight	Average rank	Frequency top model (%)
Slope	-16.61	0.92	12.31	4.8E-05	1.36	70.87
Elevation	-10.29	0.86	9.15	0.004	2.88	29.13
Vegetation	-7.16	0.78	7.58	4.0E-07	3.19	0
Soil moisture	-6.26	0.78	7.13	1.2E-06	3.57	0
Distance	-4.20	0.65	4.10	0.990	4.00	0

488 **4. Discussion**

489 Using complete mitochondrial genomes and low-coverage nuclear genomes from 77 giant root-rat
490 individuals, we uncovered a clear subdivision of localities in the north and the south of the species
491 range in the Bale Mountains, Ethiopia. Landscape genetic analysis identified topographic barriers
492 such as the steep slopes and elevation differences between the two regions as the main drivers of
493 population subdivision. Within regions, we did not identify any clear spatial structuring, suggesting a
494 high level of gene flow when topographic barriers are absent.

495

496 **Genetic subdivision between regions**

497 The significant north and south geographic subdivision in the mitochondrial and nuclear genomes,
498 was evidenced, for instance, by a high number of substitutions separating the divergent

499 mitochondrial lineages present in each region, or by the nuclear PCA analysis (Figure 2, supporting
500 information Figure S1). However, two giant root-rat individuals sampled in the south were
501 mitochondrially more closely related to their northern counterparts than their source region, which
502 may indicate ancient gene flow. Despite their closer relationship, both had a large number of
503 substitutions distinguishing them from the rest of the northern individuals, suggesting that ancestral
504 mitochondrial lineages may be retained in those two individuals that are also present in the north - a
505 remnant of their shared evolutionary history. The phylogeny indicated these two southern
506 individuals as basal to each of two distinct haplogroups found in the north, suggesting the lineages
507 were derived from two distinct divergence events. Ancient lineage retention in the south was
508 supported by our nuclear analysis, which found no evidence of recent or past gene flow between
509 north and south (Figures 2D, 3).

510 The presence of genetically distinct subpopulations may be attributed to long-lasting extrinsic
511 barriers, which prevent genetic exchange between them (Avise, 2000; Bryja et al., 2010). Slope and
512 elevation were identified as the primary drivers of genetic differentiation in our landscape analysis,
513 and in combination they presumably cause the genetic subdivision between regions (Table 1,
514 supporting information Table S4), similar to what has been observed in other fossorial rodents such
515 as the Brazilian tuco tuco of the dunes (*Ctenomys flamarioni*), or the common water vole (*Arvicola*
516 *terrestris*) (Berthier et al., 2005; Fernández-Stolz et al., 2007). The south comprises the Sanetti
517 Plateau, which is ~300 – 500 m higher in altitude than the northern region (Figure 1C) and the
518 plateau margins northwards are characterised by broad valleys with steep slopes covered by dense
519 *Erica* thickets. In addition to the slopes which themselves act as a barrier, the *Erica* thickets may
520 further limit the dispersal of the species (Miehe & Miehe, 1994; Yalden, 1985). Giant root-rats are
521 adapted to open grasslands with low vegetation and avoid dense shrubs such as *Erica*, likely due to
522 the difficulties of burrowing in woody ground and the absence of food-plants. Additionally, the
523 plateau is bounded by congealed lava flows of unknown age to the northwest. These barriers to

524 dispersal and the fossorial lifestyle of the giant root-rat limiting the species' ability to traverse
525 pronounced topographic structures, presumably caused the strong genetic subdivision of the species.
526 Our landscape genetic result is in agreement with recent satellite-based mapping of the giant-root
527 rat's distribution, which found that the texture of the landscape is the most critical factor in
528 explaining the species' range (Wraase et al., 2022).

529 In addition to slope and elevation, the pronounced subdivision observed in giant root-rats may
530 also have been reinforced by glacial extents during the Late Pleistocene. The Bale Mountains are
531 currently ice-free, but the Sanetti Plateau, the south region, was glaciated between ~42,000 to
532 16,000 years ago (kya) (Figure 1C; Groos et al., 2021; Ossendorf et al., 2019). Except for this last
533 glacial extent, exposure ages of moraines in the valleys in the northwestern part of the plateau (up to
534 ~100 kya), and stone stripes close the mountain Tullu Dimtu (up to ~360 kya) could be interpreted in
535 favour of earlier glacial periods (Groos et al., 2021). Possibly, giant root-rat individuals in the south
536 were pushed towards the outer margins of the plateau by the glaciers, which increased the
537 separation to the individuals in the north. As the glaciers retreated, colonisation of the central
538 plateau from a more southern Late Pleistocene refugium may explain the significantly lower diversity
539 in the central localities (S1 and S2) in comparison to the south eastern ones (S3, S5, S6, supporting
540 information Table S3). This would be in agreement with the often-proposed hypothesis that
541 populations of mammals exhibit reduced genetic diversity on recently deglaciated land (e.g. Hewitt,
542 1996, 2004). The glacial extent in the north and northwestern valleys of the plateau margins
543 persisted until ~16,000 years ago, while the ice shield on the plateau around Tullu Dimtu was smaller
544 in extent already ~20,000 years ago (Groos et al., 2021).

545 Although vegetation and soil moisture were previously identified as essential factors influencing
546 the local abundance of giant root-rats (Asefa et al., 2022; Šklíba et al., 2017), our study did not
547 indicate any effect on genetic differentiation (Table 1), suggesting these factors play less of a role in
548 hindering gene flow at the range-wide scale. However, the spatially coarse vegetation and soil

549 moisture indices used in our analysis may not fully capture the highly specific food and soil
550 requirements of the giant root-rat. Their primary food resource is *Alchemilla* (Yaba et al., 2011). The
551 vegetation index, which is based on remotely-derived satellite data, may not distinguish its spectral
552 signal from other non-preferred plants (Wraase et al., 2022). Additionally, the giant root-rat requires
553 soil layers of approximately 50 cm in depth to engineer burrow systems and for thermoregulation
554 (Sillero-Zubiri et al., 1995; Šumbera et al., 2020), and while soil depth and moisture are likely
555 correlated (deeper soil can store more water, Tromp-van Meerveld & McDonnell, 2006), soil
556 moisture as a proxy for soil availability may not capture areas of sufficient soil depth. The vegetation
557 and soil moisture indices were derived from a Sentinel-2 scene captured in December, just after the
558 rainy season. During this period, vegetation is still lush and green and the soil is moist across large
559 parts in the Bale Mountains National Park, and this thus might not fully reveal the specific habitat
560 requirements (related to its preference for moorlands and wet grasslands with good soil depth) of
561 the giant root-rat at that time of the year.
562
563 **Gene flow within regions**
564 We observed a lack of structuring among localities within both regions. Levels of differentiation were
565 low, with nuclear F_{ST} - estimates of 0.01-0.02 within regions, which is considered as weak
566 differentiation for nuclear data (Figure 4; Weir & Cockerham, 1984; Wright, 1978). This indicates high
567 level of dispersal and gene flow across distances of at least 16 km, which was the maximum distance
568 between two sampling localities within regions. The ability of giant root-rats to disperse across such
569 relatively large distances was in contrast to our expectations; giant root-rats are fossorial, solitary
570 and territorial. We had expected this, in combination with the heterogeneity in soil structure and
571 food availability across its range, would lead to stronger genetic structuring at small spatial scales,
572 similar to what has been observed in other fossorial rodents (Mapelli et al., 2012; Schweizer et al.,
573 2007). Although direct observations for this are still lacking, the limited substructuring within regions

574 and the large dispersal distances suggest that giant root-rats can disperse aboveground and for
575 relatively large distances. In fact, giant root-rats show morphological adaptations to surface activity,
576 in that their eyes are situated dorsally on the head, which allows them to detect predators in open
577 habitats (Yalden, 1985). In support of our findings, radio tracking has evidenced the dispersal of a
578 giant root-rat individual over a distance of up to 270 m within a span of two days; the tracked
579 individual traversed across damp soil, suggesting it did not disperse underground (Šklíba et al., 2020).
580 Aboveground dispersal has also been documented in other fossorial, solitary rodent species, such as
581 blind mole-rats (*Spalax microphthalmus*; Zagorodniuk et al., 2018) and Tibetan plateau zokors
582 (*Eospalax fontanieri*; Chu et al., 2021). Even in strictly subterranean African mole-rats, long-distance
583 dispersal is not precluded (*Fukomys damarensis*, Bathyergidae; Finn et al., 2022). For giant root-rats,
584 aboveground dispersal attempts could be triggered by decreasing food supply, the absence of sexual
585 partners, or the presence of competitors (Šklíba et al., 2020; Zagorodniuk et al., 2018). Also, the
586 behaviour may circumvent the patchy availability of suitable habitats and small home-ranges,
587 maintaining gene flow and limiting genetic structuring across small spatial scales.

588 Dispersal events in the giant root-rat may be male-dominated, as it has been observed in tuco
589 tucos (*Ctenomys talarum* and *C. australis*; Cutrera et al., 2005; Mora et al., 2010), Chinese zokor
590 (*Eospalax fontanierii*, Zhang, 2007), giant mole-rats (*F. mechowii*; Kawalika & Burda, 2007), and
591 arvicoline rodents (Le Galliard et al., 2012). While sex-specific dispersal has not been studied in the
592 giant root-rat yet, the observation of males being more frequently involved in dispersal attempts
593 compared to females (Šklíba et al., 2020) and that microsatellite analysis also indicate that males
594 disperse for longer distances (Dovičicová et al. in prep.) suggests that this type of dispersal may be
595 prevalent in the species.

596 Our nuclear data did suggest slight subdivision in the south, with localities in the central part of
597 the plateau (S1, S2) being more differentiated from localities in the southeast (S3-S6; Figure 1C). This
598 was evidenced by increased F_{ST} in their pairwise comparisons and their segregation on the second

599 principal component on the PCA (Figure 2C, D). Although overall differentiation among localities in
600 the south were low, this pattern may reflect topographic features; the mountain Tullu Dimtu, the
601 highest peak in the Bale Mountains National Park with 4,377 m a.s.l., is located close to localities S3
602 and S4, and may hinder gene flow (Figure 1C).
603
604 **Conservation implications**
605 Through landscape genetic analysis, we identified the drivers of population subdivision between
606 north and south to be topographic barriers in the form of slope and elevation. While the species is
607 capable of dispersing locally, our findings suggest that giant root-rats in the north and south must be
608 considered separately when developing conservation strategies, as there is no opportunity for
609 dispersal and gene flow between them. Giant root-rat impact their surrounding environment as
610 ecosystem engineers and primary prey for the endangered Ethiopian wolf, which underscores the
611 importance of their persistence (Sillero-Zubiri & Gottelli, 1995; Šklíba et al., 2017). Already, the giant
612 root-rat is believed to have a small census size due to its limited distribution range (although no
613 census estimate is available), and is listed as endangered by the IUCN (Lavrenchenko & Kennerley,
614 2016). The potential for reduction of the species' distribution range due to increasing human
615 activities in the form of expanding livestock grazing and human settlements in the Bale Mountains,
616 could harm the species' persistence with negative consequences for the overall ecological balance in
617 the region (Gashaw, 2015; Mekonen, 2020; Stephens et al., 2001). Our study yields some key insights
618 for planning future conservation strategies for the species and highlights the value of genomic data
619 in expanding our understanding of the population dynamics and environmental features that drive
620 the structuring of range-limited fossorial species. With ongoing environmental changes, it is crucial to
621 utilize this knowledge to safeguard mountain biodiversity and ecosystem functioning.

Acknowledgements

This work was supported by the German Research Council (DFG) in the framework of the joint Ethio-European DFG Research Unit 2358 "The Mountain Exile Hypothesis. How humans benefited from and re-shaped African high-altitude ecosystems during Quaternary climate changes" [FA-925/14-1], [OP-219/10-2] and [SCHA-2085/3-1]. We are grateful to the Ethiopian Wildlife Conservation Authority, the College of Natural and Computational Sciences (Addis Ababa University), the Department of Plant Biology and Biodiversity Management (Addis Ababa University), the Frankfurt Zoological Society, the Ethiopian Wolf Project, and the Bale Mountains National Park for their cooperation and kind permission to conduct fieldwork. We are thankful to Awol Assefa, Wege Abebe, Mohammed Ahmed Muhammed and Katinka Thielsen for contributing to the preparation and implementation of the fieldwork, Christian Lampei for input on landscape genetic analyses, Alexander Groos for the input on Late Pleistocene glaciation, and Usman Abdella, Hamza Ahmed, Mohammed Kadir, Kasim Adem, Hussein Umer and Sophie Haje, for their great assistance in the field. The research was also supported by Villum Fonden Young Investigator Programme, grant no 13151 and Independent Research Fund Denmark, Sapere Aude: DFF-Forskningsleder, grant no 9064-00025B to EDL.

References

Akaike, H. (1974). A New Look at the Statistical Model Identification. *IEEE Transactions on Automatic Control*, *19*(6), 716–723.

Alexander, A. (2017). *genetic_diversity_diffs v1.0.3*. https://github.com/laninsky/genetic_diversity_diffs

Asefa, A., Reuber, V., Miehe, G., Wondafrash, M., Wraase, L., Wube, T., Farwig, N., & Schabo, D. G. (2022). The activity of a subterranean small mammal alters Afroalpine vegetation patterns and is positively affected by livestock grazing. *Basic and Applied Ecology*.

Avise, J. C. (2000). *Phylogeography: the history and formation of species*. Havard University Press.

646 Badgley, C., Smiley, T. M., Terry, R., Davis, E. B., DeSantis, L. R. G., Fox, D. L., Hopkins, S. S. B., Jezkova,
647 T., Matocq, M. D., Matzke, N., McGuire, J. L., Mulch, A., Riddle, B. R., Roth, V. L., Samuels, J. X.,
648 Strömberg, C. A. E., & Yanites, B. J. (2017). Biodiversity and Topographic Complexity: Modern
649 and Geohistorical Perspectives. *Trends in Ecology and Evolution*, *32*(3), 211–226.
650 Begall, S., Burda, H., & Schleich, C. E. (2007). *Subterranean rodents: news from underground*.
651 Springer.
652 Berthier, K., Galan, M., Foltête, J. C., Charbonnel, N., & Cosson, J. F. (2005). Genetic structure of the
653 cyclic fossorial water vole (Arvicola terrestris): Landscape and demographic influences.
654 *Molecular Ecology*, *14*(9), 2861–2871.
655 Birky, W. C., Maruyama, T., & Fuerst, P. (1983). An approach to population and evolutionary genetic
656 theory for genes in mitochondria and chloroplasts, and some results. *Genetics*, *103*, 513–527.
657 Boulangeat, I., Gravel, D., & Thuiller, W. (2012). Accounting for dispersal and biotic interactions to
658 disentangle the drivers of species distributions and their abundances. *Ecology Letters*, *15*(6),
659 584–593.
660 Brown, J. H. (2001). Mammals on mountainsides: elevational patterns of diversity. *Global Ecology*
661 *and Biogeography*, *10*(1), 101–109.
662 Bryja, J., Granjon, L., Dobigny, G., Patzenhauerová, H., Konečný, A., Duplantier, J. M., Gauthier, P.,
663 Colyn, M., Durnez, L., Lalis, A., & Nicolas, V. (2010). Plio-Pleistocene history of West African
664 Sudanian savanna and the phylogeography of the Praomys daltoni complex (Rodentia): The
665 environment/geography/genetic interplay. *Molecular Ecology*, *19*(21), 4783–4799.
666 Carøe, C., Gopalakrishnan, S., Vinner, L., Mak, S. S. T., Sinding, M. H. S., Samaniego, J. A., Wales, N.,
667 Sicheritz-Pontén, T., & Gilbert, M. T. P. (2018). Single-tube library preparation for degraded
668 DNA. *Methods in Ecology and Evolution*, *9*(2), 410–419.
669 Chu, B., Ji, C., Zhou, J., Zhou, Y., & Hua, L. (2021). Why does the plateau zokor (Myospalax fontanieri:
670 Rodentia: Spalacidae) move on the ground in summer in the eastern Qilian Mountains? *Journal*

671 *of Mammalogy*, *102*(1), 346–357.

672 Clarke, R. T., Rothery, P., & Raybould, A. F. (2002). Confidence limits for regression relationships
673 between distance matrices: Estimating gene flow with distance. *Journal of Agricultural,*
674 *Biological, and Environmental Statistics*, *7*(3), 361–372.

675 Cunningham, H. R., Rissler, L. J., Buckley, L. B., & Urban, M. C. (2016). Abiotic and biotic constraints
676 across reptile and amphibian ranges. *Ecography*, *39*(1), 1–8.

677 Cushman, S. A., & Landguth, E. L. (2010). Spurious correlations and inference in landscape genetics.
678 *Molecular Ecology*, *19*(17), 3592–3602.

679 Cushman, S. A., & Lewis, J. S. (2010). Movement behavior explains genetic differentiation in
680 American black bears. *Landscape Ecology*, *25*(10), 1613–1625.

681 Cushman, S. A., McKelvey, K. S., Hayden, J., & Schwartz, M. K. (2006). Gene flow in complex
682 landscapes: Testing multiple hypotheses with causal modeling. *American Naturalist*, *168*(4),
683 486–499.

684 Cutrera, A. P., Lacey, E. A., & Busch, C. (2005). Genetic structure in a solitary rodent (Ctenomys
685 talarum): Implications for kinship and dispersal. *Molecular Ecology*, *14*(8), 2511–2523.

686 Davies, T. J., Purvis, A., & Gittleman, J. L. (2009). Quaternary climate change and the geographic
687 ranges of mammals. *American Naturalist*, *174*(3), 297–307.

688 Excoffier, L., & Lischer, H. E. L. (2010). Arlequin suite ver 3.5: A new series of programs to perform
689 population genetics analyses under Linux and Windows. *Molecular Ecology Resources*, *10*(3),
690 564–567.

691 Fernández-Stolz, G. P., Stolz, J. F. B., & De Freitas, T. R. O. (2007). Bottlenecks and dispersal in the
692 tuco-tuco das dunas, Ctenomys flamarioni (Rodentia: Ctenomyidae), in Southern Brazil. *Journal*
693 *of Mammalogy*, *88*(4), 935–945.

694 Finn, K. T., Thorley, J., Bensch, H. M., & Zöttl, M. (2022). Subterranean Life-Style Does Not Limit Long
695 Distance Dispersal in African Mole-Rats. *Frontiers in Ecology and Evolution*, *10*.

696 Gashaw, T. (2015). Threats of Bale Mountains National Park and solutions, Ethiopia. *Journal of*
697 *Physical Science and Environmental Studies*, *1*(2), 10–16.
698 Gaston, K. J. (2003). *The stucture and dynamics of geographic ranges*. Oxford University Press.
699 Groos, A. R., Akçar, N., Yesilyurt, S., Miehe, G., Vockenhuber, C., & Veit, H. (2021). Nonuniform late
700 pleistocene glacier fluctuations in tropical Eastern Africa. *Science Advances*, *7*(11).
701 Guo, Y. T., Zhang, J., Xu, D. M., Tang, L. Z., & Liu, Z. (2021). Phylogenomic relationships and molecular
702 convergences to subterranean life in rodent family Spalacidae. *Zoological Research*, *42*(5), 671–
703 674.
704 Harestad, A. S., & Bunnel, F. L. (1979). Home Range and Body Weight--A Reevaluation. *Ecology*, *60*(2),
705 389–402.
706 Hewitt, G. M. (1996). Some genetic consequences of ice ages, and their role in divergence and
707 speciation. *Biological Journal of the Linnean Society*, *58*(3), 247–276.
708 Hewitt, G. M. (2004). The structure of biodiversity - Insights from molecular phylogeography.
709 *Frontiers in Zoology*, *1*, 1–16.
710 Hoffmann, A. A., Sgrò, C. M., & Kristensen, T. N. (2017). Revisiting Adaptive Potential, Population
711 Size, and Conservation. *Trends in Ecology and Evolution*, *32*(7), 506–517.
712 Kawalika, M., & Burda, H. (2007). Giant Mole-rats, Fukomys mechowii, 13 Years on the Stage. In S.
713 Begall, H. Burda, & C. E. Schleich (Eds.), *Subterranean Rodents: News from Underground* (pp.
714 205–219). Springer.
715 Korneliussen, T. S., Albrechtsen, A., & Nielsen, R. (2014). ANGSD: Analysis of Next Generation
716 Sequencing Data. *BMC Bioinformatics*, *15*(1), 1–13.
717 Lande, R. (1988). Genetics and demography in biological conservation. *Science*, *241*(4872), 1455–
718 1460.
719 Lanfear, R., Frandsen, P. B., Wright, A. M., Senfeld, T., & Calcott, B. (2017). Partitionfinder 2: New
720 methods for selecting partitioned models of evolution for molecular and morphological

721 phylogenetic analyses. *Molecular Biology and Evolution*, *34*(3), 772–773.

722 Lavrenchenko, L., & Kennerley, R. (2016). *Tachyoryctes macrocephalus, The IUCN Red List of*
723 *Threatened Species 2016: e.T21293A115161321*.

724 Le Galliard, J. F., Rémy, A., Ims, R. A., & Lambin, X. (2012). Patterns and processes of dispersal
725 behaviour in arvicoline rodents. *Molecular Ecology*, *21*(3), 505–523.

726 Leigh, J. W., & Bryant, D. (2015). POPART: Full-feature software for haplotype network construction.
727 *Methods in Ecology and Evolution*, *6*(9), 1110–1116.

728 Li, H., & Durbin, R. (2009). Fast and accurate short read alignment with Burrows–Wheeler transform.
729 *Bioinformatics*, *25*(14), 1754–1760.

730 Li, H., Handsaker, B., Wysoker, A., Fennell, T., Ruan, J., Homer, N., Marth, G., Abecasis, G., & Durbin,
731 R. (2009). The Sequence Alignment/Map format and SAMtools. *Bioinformatics*, *25*(16), 2078–
732 2079.

733 Magoč, T., & Salzberg, S. L. (2011). FLASH: Fast length adjustment of short reads to improve genome
734 assemblies. *Bioinformatics*, *27*(21), 2957–2963.

735 Manel, S., Gugerli, F., Thuiller, W., Alvarez, N., Legendre, P., Holderegger, R., Gielly, L., & Taberlet, P.
736 (2012). Broad-scale adaptive genetic variation in alpine plants is driven by temperature and
737 precipitation. *Molecular Ecology*, *21*(15), 3729–3738.

738 Mapelli, F. J., Mora, M. S., Mirol, P. M., & Kittlein, M. J. (2012). Population structure and landscape
739 genetics in the endangered subterranean rodent Ctenomys porteousi. *Conservation Genetics*,
740 *13*(1), 165–181.

741 Meisner, J., & Albrechtsen, A. (2018). Inferring Population Structure and Admixture Proportions in
742 Low-Depth NGS Data. *Genetics*, *210*(2), 719–731.

743 Mekonen, S. (2020). Coexistence between human and wildlife: The nature, causes and mitigations of
744 human wildlife conflict around Bale Mountains National Park, Southeast Ethiopia. *BMC Ecology*,
745 *20*(1), 1–9.

746 Miehe, S., & Miehe, G. (1994). Ericaceous forests and heathlands in the Bale Mountains of South
747 Ethiopia. In *Ecology and Man's Impact*. Traute Warnke, Hamburg.
748 Mirol, P., Giménez, M. D., Searle, J. B., Bidau, C. J., & Faulkes, C. G. (2010). Population and species
749 boundaries in the South American subterranean rodent Ctenomys in a dynamic environment.
750 *Biological Journal of the Linnean Society*, *100*(2), 368–383.
751 Mora, M. S., Mapelli, F. J., Gaggiotti, O. E., Kittlein, M. J., & Lessa, E. P. (2010). Dispersal and
752 population structure at different spatial scales in the subterranean rodent Ctenomys australis.
753 *BMC Genetics*, *11*(9).
754 Nevo, E. (1999). *Mosaic evolution of subterranean mammals: regression, progression and global*
755 *convergence*. Oxford Univ Press.
756 Oksanen, J., Legendre, P., O'Hara, B., Stevens, M. H. H., Oksanen, M. J., & Suggests, M. (2020). Vegan:
757 Community Ecology Package. R package version 2.5-7. In *Community ecology package* (Vol. 10,
758 pp. 631–637).
759 Ossendorf, G., Groos, A. R., Bromm, T., Tekelemariam, M. G., Glaser, B., Lesur, J., Schmidt, J., Akçar,
760 N., Bekele, T., Beldados, A., Demissew, S., Kahsay, T. H., Nash, B. P., Nauss, T., Negash, A.,
761 Nemomissa, S., Veit, H., Vogelsang, R., Woldu, Z., … Miehe, G. (2019). Middle Stone Age
762 foragers resided in high elevations of the glaciated Bale Mountains, Ethiopia. *Science*,
763 *365*(6453), 583–587.
764 Parmesan, C. (2006). Ecological and evolutionary responses to recent climate change. In *Annual*
765 *Review of Ecology, Evolution, and Systematics* (Vol. 37, pp. 637–669). Annual Reviews.
766 Peterman, W. E. (2018). ResistanceGA: An R package for the optimization of resistance surfaces using
767 genetic algorithms. *Methods in Ecology and Evolution*, *9*(6), 1638–1647.
768 Peterman, W. E., Connette, G. M., Semlitsch, R. D., & Eggert, L. S. (2014). Ecological resistance
769 surfaces predict fine-scale genetic differentiation in a terrestrial woodland salamander.
770 *Molecular Ecology*, *23*(10), 2402–2413.

771 Quaglietta, L., Fonseca, V. C., Hájková, P., Mira, A., & Boitani, L. (2013). Fine-scale population genetic
772 structure and short-range sex-biased dispersal in a solitary carnivore, Lutra lutra. *Journal of*
773 *Mammalogy*, *94*(3), 561–571.
774 R Core Team. (2021). *R: A Language and Environment for Statistical Computing. R Foundation for*
775 *Statistical Computing*. https://www.r-project.org/
776 Rahbek, C., Borregaard, M. K., Antonelli, A., Colwell, R. K., Holt, B. G., Nogues-Bravo, D., Rasmussen,
777 C. M. Ø., Richardson, K., Rosing, M. T., Whittaker, R. J., & Fjeldså, J. (2019). Building mountain
778 biodiversity: Geological and evolutionary processes. *Science*, *365*(6458), 1114–1119.
779 Rahbek, C., Borregaard, M. K., Colwell, R. K., Dalsgaard, B., Holt, B. G., Morueta-Holme, N., Nogues-
780 Bravo, D., Whittaker, R. J., & Fjeldså, J. (2019). Humboldt's enigma: What causes global patterns
781 of mountain biodiversity? *Science*, *365*(6458), 1108–1113.
782 Reichman, O. J. (1975). Relation of Desert Rodent Diets to Available Resources. *Journal of*
783 *Mammalogy*, *56*(4), 731–751. https://doi.org/10.2307/1379649
784 Reuber, V. M., Rey-Iglesia, A., Westbury, M. V., Cabrera, A. A., Farwig, N., Skovrind, M., Šumbera, R.,
785 Wube, T., Opgenoorth, L., Schabo, D. G., & Lorenzen, E. D. (2021). Complete mitochondrial
786 genome of the giant root-rat (Tachyoryctes macrocephalus). *Mitochondrial DNA Part B:*
787 *Resources*, *6*(8), 2191–2193.
788 Rice, W. R. (1989). Analyzing tables of statistical tests. *Evolution*, *43*, 223–225.
789 Ronquist, F., & Huelsenbeck, J. P. (2003). MrBayes 3: Bayesian phylogenetic inference under mixed
790 models. *Bioinformatics*, *19*(12), 1572–1574.
791 Rousset, F. (1997). Genetic differentiation and estimation of gene flow from F-statistics under
792 isolation by distance. *Genetics*, *145*(4), 1219–1228.
793 Rozas, J., Sánchez-DelBarrio, J. C., Messeguer, X., & Rozas, R. (2003). DnaSP, DNA polymorphism
794 analyses by the coalescent and other methods. *Bioinformatics*, *19*(18), 2496–2497.
795 Ruiz-Gonzalez, A., Cushman, S. A., Madeira, M. J., Randi, E., & Gómez-Moliner, B. J. (2015). Isolation

by distance, resistance and/or clusters? Lessons learned from a forest-dwelling carnivore inhabiting a heterogeneous landscape. *Molecular Ecology*, *24*(20), 5110–5129.

Sandel, B., Arge, L., Dalsgaard, B., Davies, R. G., Gaston, K. J., Sutherland, W. J., & Svenning, J. C. (2011). The influence of late quaternary climate-change velocity on species endemism. *Science*, *334*(6056), 660–664.

Schweizer, M., Excoffier, L., & Heckel, G. (2007). Fine-scale genetic structure and dispersal in the common vole (Microtus arvalis). *Molecular Ecology*, *16*(12), 2463–2473.

Scrucca, L. (2013). GA: A Package for Genetic Algorithms in R. *Journal of Statistical Software*, *53*(4), 1–37.

Sexton, J. P., McIntyre, P. J., Angert, A. L., & Rice, K. J. (2009). Evolution and ecology of species range limits. *Annual Review of Ecology, Evolution, and Systematics*, *40*, 415–436.

Shirk, A. J., Landguth, E. L., & Cushman, S. A. (2018). A comparison of regression methods for model selection in individual-based landscape genetic analysis. *Molecular Ecology Resources*, *18*(1), 55–67.

Sillero-Zubiri, C., & Gottelli, D. (1995). Diet and Feeding Behavior of Ethiopian Wolves (Canis simensis). *Journal of Mammalogy*, *76*(2), 531–541.

Sillero-Zubiri, C., Tattersall, F. H., & Macdonald, D. W. (1995). Habitat selection and daily activity of giant molerats Tachyoryctes macrocephalus: Significance to the Ethiopian wolf Canis simensis in the Afroalpine ecosystem. *Biological Conservation*, *72*(1), 77–84.

Šklíba, J., Vlasatá, T., Lövy, M., Hrouzková, E., Meheretu, Y., Sillero-Zubiri, C., & Šumbera, R. (2017). Ecological role of the giant root-rat (Tachyoryctes macrocephalus) in the Afroalpine ecosystem. *Integrative Zoology*, *12*(4), 333–344.

Šklíba, J., Vlasatá, T., Lövy, M., Hrouzková, E., Meheretu, Y., Sillero-Zubiri, C., & Šumbera, R. (2020). The giant that makes do with little: small and easy-to-leave home ranges found in the giant root-rat. *Journal of Zoology*, *310*(1), 64–70.

821 Skotte, L., Korneliussen, T. S., & Albrechtsen, A. (2013). Estimating individual admixture proportions
822 from next generation sequencing data. *Genetics*, *195*(3), 693–702.
823 Stephens, P. A., D'Sa, C. A., Sillero-Zubiri, C., & Leader-Williams, N. (2001). Impact of livestock and
824 settlement on the large mammalian wildlife of Bale Mountains National Park, southern
825 Ethiopia. *Biological Conservation*, *100*(3), 307–322.
826 Šumbera, R., Lövy, M., Marino, J., Šimek, M., & Šklíba, J. (2020). Gas composition and its daily
827 changes within burrows and nests of an Afroalpine fossorial rodent, the giant root-rat
828 Tachyoryctes macrocephalus. *Zoology*, *142*, 125819.
829 Tallents, L. A., & Macdonald, D. W. (2011). Mapping High-Altitude Vegetation in the Bale Mountains,
830 Ethiopia. *Walia—Special Edition on the Bale Mountains*, 97–117.
831 Tromp-van Meerveld, H. J., & McDonnell, J. J. (2006). On the interrelations between topography, soil
832 depth, soil moisture, transpiration rates and species distribution at the hillslope scale. *Advances*
833 *in Water Resources*, *29*(2), 293–310.
834 Tucker, M. A., Ord, T. J., & Rogers, T. L. (2014). Evolutionary predictors of mammalian home range
835 size: Body mass, diet and the environment. *Global Ecology and Biogeography*, *23*(10), 1105–
836 1114.
837 Vlasatá, T., Šklíba, J., Lövy, M., Meheretu, Y., Sillero-Zubiri, C., & Šumbera, R. (2017). Daily activity
838 patterns in the giant root rat (Tachyoryctes macrocephalus), a fossorial rodent from the Afro-
839 alpine zone of the Bale Mountains, Ethiopia. *Journal of Zoology*, *302*(3), 157–163.
840 Weir, B. S., & Cockerham, C. C. (1984). *Estimating F-Statistics for the Analysis of Population Structure*.
841 *38*(6), 1358–1370.
842 Westbury, M. V., Hartmann, S., Barlow, A., Wiesel, I., Leo, V., Welch, R., Parker, D. M., Sicks, F.,
843 Ludwig, A., Dalen, L., & Hofreiter, M. (2018). Extended and Continuous Decline in Effective
844 Population Size Results in Low Genomic Diversity in the World's Rarest Hyena Species, the
845 Brown Hyena. *Molecular Biology and Evolution*, *35*(5), 1225–1237.

Willi, Y., Van Buskirk, J., & Hoffmann, A. A. (2006). Limits to the adaptive potential of small populations. *Annual Review of Ecology, Evolution, and Systematics*, *37*, 433–458.

Wilson, R. J., & Gutiérres, D. (2016). Effects of Climate Change on the Elevational Limits of Species Ranges. In *Ecological Consequences of Climate Change: Mechanisms, Conservation, and Management* (pp. 107–132).

Wraase, L., Reuber, V. M., Kurth, P., Fekadu, M., Demissew, S., Miehe, G., Opgenoorth, L., Selig, U., Woldu, Z., Zeuss, D., Schabo, D. G., Farwig, N., & Nauss, T. (2022). Remote sensing-supported mapping of the activity of a subterranean landscape engineer across an afro-alpine ecosystem. *Remote Sensing in Ecology and Conservation*, 1–15.

Wright, S. (1969). *Evolution and the genetics of populations, vol. 2, The Theory of Gene Frequencies*. University of Chicago Press.

Wright, S. (1978). *Evolution and the genetics of populations, vol. 4: variability within and among natural populations*. University of Chicago Press.

Yaba, M., Mekonnen, T., Bekele, A., & Malcolm, J. (2011). Food selection and feeding behavior of giant mole rat (Tachyoryctes macrocephalus, Ruppell, 1842) from the sanetti plateau of bale mountains national park, Ethiopia. In *Asian Journal of Applied Sciences* (Vol. 4, Issue 7, pp. 735–740).

Yalden, D. W. (1985). Tachyoryctes macrocephalus. *Mammalian Species*, *237*, 1–3.

Yalden, D. W., & Largen, M. J. (1992). The endemic mammals of Ethiopia. *Mammal Review*, *22*(3–4), 115–150.

Zagorodniuk, I., Korobchenko, M., Parkhomenko, V., & Barkaszi, Z. (2018). Steppe rodents at the edge of their range: A case study of Spalax microphthalmus in the north of Ukraine. *Biosystems Diversity*, *26*(3), 188–200.

Zhang, Y. (2007). The Biology and Ecology of Plateau Zokors (Eospalax fontanierii). In S. Begall, H. Burda, & C. E. Schleich (Eds.), *Subterranean Rodents: News from Underground* (pp. 237–249).

871 Springer.

872

873 **Data accessibility and benefit-sharing statement**

874 Data accessibility: The mitochondrial genome data that support the findings of this study will be
875 openly available in GenBank of NCBI at https://www.ncbi.nlm.nih.gov under accession no.
876 OQ207545-OQ207620 and MW751806, upon acceptance of this paper. The raw sequencing reads
877 will be available in the associated BioProject PRJNA940645.
878 Benefit sharing: This project was designed as a joint Ethio-European research collaboration and
879 developed with scientists from Ethiopia that provided the genetic samples. Our project is committed
880 to international scientific partnerships and our collaborators are included as co-authors. The research
881 addresses a priority concern, in this case the conservation of the studied organism.

882 **Author contributions**

883 NF, GM, LO, TW and DGS designed the research concept and NF, LO and DGS secured the project
884 funding. VMR, AA, LW and DGS captured specimens in the field. VMR and AR-I conducted lab work.
885 VMR, AR-I and MVW analysed the data with contributions from RS, EDL, and DGS for genetic and
886 ecological interpretation. LW generated raster layers for landscape genetic analyses. VMR, EDL and
887 DGS wrote the manuscript with contributions from all co-authors. All authors gave final approval for
888 publication and agreed to be held accountable for the work carried out within this publication.